MECSOL 2022 - Proceedings of the 8th International Symposium on Solid Mechanics
M.L. Bittencourt, J. Labaki, L.C.M. Vieira Jr. and E. Mesquita (Editors), Campinas SP, Brazil, October 17th to 19th, 2022

The Finite Element Method applied to the numerical modelling of in-plane and out-of-plane Stress fields in Laminated Composite Reissner-Mindlin Plates

Marcos Antonio Riquetto Ezequiel[1], Carlos Henrique Daros[1]

[1]Departamento de Mecânica Computacional, UNICAMP, Rua Mendeleyev 200, 13083-860, Cidade Universitária - Campinas, Brazil

Abstract. A non-linear finite element analysis is considered here for the static modeling of Symmetric Laminated Composite Reissner-Mindlin Plates. Composite Laminated Plates are composed of layers with different fibers' orientations. Such plates can be tailored for specific applications and are used extensively in the aerospace industry. We consider here a geometric nonlinearity for the plate in the form of small strains and moderate rotations (von Kármán nonlinearity). The in-plane stresses for both linear and nonlinear solutions are obtained from the von Kármán strain terms. The interlaminar (out-of-plane) stresses for the linear solution are recovered directly from the linear equilibrium equations. Results are validated e.g. using 3D analytical solutions for full supported plates. Additionally, a revision of available strategies to obtain the interlaminar stresses for the non-linear case is also considered here. Besides shear locking effects that may affect the Reissner-Mindlin Plate Theory, the axial bending coupling, inherent to the geometric nonlinearity, may produce additional membrane locking. Reduced integration will be applied to circumvent all locking effects.

Keywords:Laminated Composites, Interlaminar stress, Nonlinear finite element method, Reissner-Mindlin plates

INTRODUCTION

The use of composite materials has increased constantly in various industries over the last years, having replaced other materials such aluminum as a major structural component in the aerospace and automotive applications due to its high specific strength (Hartman, 2013). Generally fibers with high stiffness are fixed in a matrix to form a composite material, which may present a degree of anisotropy. Stacking this laminae together creates a laminated composite. The laminae can be oriented in any desired direction grating the designer the freedom to tailor the material stiffness and strength. One example that illustrates the importance of composite materials is the Boeing 787 Dreamliner, as shown on Fig.1 50% of its skin structure is made of composite materials.

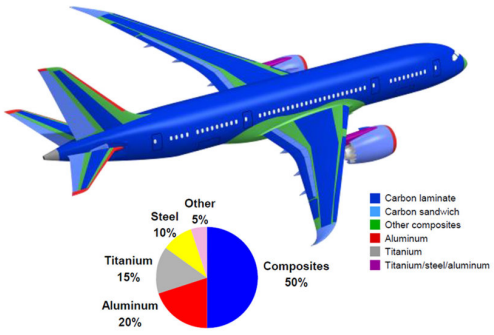

Figure 1 – Boeing 717 Dreamliner skin structure.

There are several theories for the modeling of stress field on plates. Among them we can cite *classical laminate plate theory* (CLPT), that uses the Kirchhoff hypothesis, resulting in zero transverse strains and the Reissner-Mindlin plate theory that considers a constant shear strain trough the plates thickness. Because of their relatively cheap computational

cost when compared to higher order plate theories and 3D methods, they are vastly used. The problem with the use of these plate theories on the analysis of laminated composite plates, is that different material properties between layers may lead to complex stress distributions, which may cause delamination (Patton et al., 2020). So for the failure analysis of these materials, the interlaminar shear and normal stresses are essential.
To keep the advantages of the 2D plate theories and solve the laminated composite plate problem the equilibrium equations were applied on the in plane stress field of these theories in order to recover the out of plane stresses. Pagano (1970) compared the results of stress recovery on the CLPT with his analytical linear elasticity solution for simply-supported plates, and achieved excellent results for high span ratios. Non-linear analysis, is another important point when the topic of weight reduction is taken into account. The von Kármán geometric nonlinearity is a common way to analyse the displacement field on plates with small strains and small to moderate rotation. As the load on a plate increases it starts developing internal forces that resist deformation. The larger the deformation the larger this internal forces become, and so the stiffness of the plate. So the nonlinear analysis grants a more accurate limit to the material.

FORMULATION

The Non-linear *first order shear deformation theory* (FSDT) plate Finite Element utilized in this paper was proposed by Reddy (2004), which uses a *equivalent-single-layer* (ESL) 2D theory to estimate the laminated composite plate behavior. Small strain and moderate rotations will be considered by the inclusion of the von Kármán non-linearity. The interlaminar stresses for the linear solution are recovered using the linear equilibrium equations. It is also assumed that in view of the small strain, it is not necessary to distinguish between deformed and undeformed coordinates

Plate Theory

The FSDT states that a plane section perpendicular to the main mid-surface of a plate in the undeformed remains straight and inextensible. From these assumptions we are able to derive the displacement field:

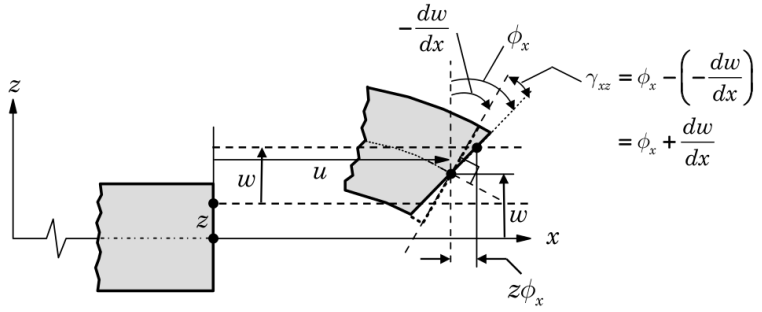

Figure 2 – Kinematics of a FSDT plate (Reddy, 2014).

$$u_1(x,y,z) = u(x,y) + z\phi_x(x,y), \quad u_2(x,y,z) = v(x,y) + z\phi_y(x,y), \quad u_3(x,y,z) = w(x,y) \tag{1}$$

where (u,v,w) are the mid-plane displacements and (ϕ_x,ϕ_y) are the rotations of a transverse plane.

From Eq. (1) we get the von Kármán strains:

$$\left\{\begin{array}{c}\varepsilon_{xx}\\ \varepsilon_{yy}\\ \gamma_{yz}\\ \gamma_{xz}\\ \gamma_{xy}\end{array}\right\} = \left\{\begin{array}{c}\varepsilon^0_{xx}\\ \varepsilon^0_{yy}\\ \gamma^0_{yz}\\ \gamma^0_{xz}\\ \gamma^0_{xy}\end{array}\right\} + z\left\{\begin{array}{c}\varepsilon^1_{xx}\\ \varepsilon^1_{yy}\\ 0\\ 0\\ \gamma^1_{xy}\end{array}\right\} = \left\{\begin{array}{c}\frac{\partial u}{\partial x} + \frac{1}{2}\left(\frac{\partial w}{\partial x}\right)^2\\ \frac{\partial v}{\partial y} + \frac{1}{2}\left(\frac{\partial w}{\partial y}\right)^2\\ \frac{\partial w}{\partial y} + \phi_y\\ \frac{\partial w}{\partial x} + \phi_x\\ \frac{\partial u}{\partial y} + \frac{\partial v}{\partial x} + \frac{\partial w}{\partial x}\frac{\partial w}{\partial y}\end{array}\right\} + z\left\{\begin{array}{c}\frac{\partial \phi_x}{\partial x}\\ \frac{\partial \phi_y}{\partial y}\\ 0\\ 0\\ \frac{\partial \phi_x}{\partial y} + \frac{\partial \phi_y}{\partial x}\end{array}\right\} \tag{2}$$

A thin to moderately thick plate may be considered to be in a state of plane stress so the in plane stress field may be

determined by the constitutive relations:

$$\left\{ \begin{array}{c} \sigma_{xx} \\ \sigma_{yy} \\ \sigma_{xy} \end{array} \right\} = \left[\begin{array}{ccc} Q_{11}^k & Q_{12}^k & 0 \\ Q_{12}^k & Q_{22}^k & 0 \\ 0 & 0 & Q_{66}^k \end{array} \right] \left\{ \begin{array}{c} \varepsilon_{xx} \\ \varepsilon_{yy} \\ \gamma_{xy} \end{array} \right\} \tag{3}$$

and the out of plane stresses are given by:

$$\left\{ \begin{array}{c} \sigma_{yz} \\ \sigma_{xz} \end{array} \right\} = \left[\begin{array}{cc} Q_{44}^k & 0 \\ 0 & Q_{55}^k \end{array} \right] \left\{ \begin{array}{c} \gamma_{yz} \\ \gamma_{xz} \end{array} \right\} \tag{4}$$

where the k index is to account for the different layer properties and the Q_{ij}^k plane stress-reduced stifness are given by:

$$\begin{array}{ll} Q_{11}^k = \frac{E_1^k}{1-\nu_{12}^k \nu_{21}^k}, & Q_{12}^k = \frac{\nu_{12}^k E_2^k}{1-\nu_{12}^k \nu_{21}^k} = \frac{\nu_{21}^k E_1^k}{1-\nu_{12}^k \nu_{21}^k} \\ Q_{22}^k = \frac{E_2^k}{1-\nu_{12}^k \nu_{21}^k}, & Q_{66}^k = G_{12}^k, \quad Q_{44}^k = G_{23}^k, \quad Q_{55}^k = G_{13}^k \end{array} \tag{5}$$

Stress Recovery

As discussed before by using the equilibrium equations from the 3D linear elasticity we are able to recover the out of plane stresses from the in plane stresses. The equilibrium equations can be expressed as:

$$\sigma_{xx,x} + \sigma_{xy,y} + \sigma_{xz,z} = -b_1 \qquad \sigma_{xy,x} + \sigma_{yy,y} + \sigma_{yz,z} = -b_2 \qquad \sigma_{xz,x} + \sigma_{yz,y} + \sigma_{zz,z} = -b_3 \tag{6}$$

We consider here that there are no body forces, so (b_1, b_2, b_3) are zero. The in plane stress relations given by Eqs. (2) and (3) can them be substituted on Eq. (6) resulting in:

$$\begin{aligned} \sigma_{xz}(z) &= -\int_{\bar{z}}^{z} \left(Q_{11}^k \left(u_{,xx} + z\phi_{x,xx} \right) + Q_{12}^k \left(u_{,yy} + v_{,xy} + z\left(\phi_{x,yy} + \phi_{y,xy} \right) \right) \right) \mathrm{d}z + \sigma_{xz}(\bar{z}) \\ \sigma_{yz}(z) &= -\int_{\bar{z}}^{z} \left(Q_{12}^k \left(u_{,xy} + v_{,xx} + z\left(\phi_{x,xy} + \phi_{y,xx} \right) \right) + Q_{22}^k \left(v_{,yy} + z\phi_{y,yy} \right) \right) \mathrm{d}z + \sigma_{yz}(\bar{z}) \\ \sigma_{zz}(z) &= \int_{\bar{z}}^{z} \left[\int_{\bar{z}}^{\zeta} \left(Q_{11}^k \left(u_{,xxx} + z\phi_{x,xxx} \right) + Q_{22}^k \left(v_{,yyy} + z\phi_{y,yyy} \right) + 2Q_{12}^k \left(u_{,xyy} + v_{,xxy} + \right. \right. \right. \\ &\quad \left. \left. \left. z\left(\phi_{x,xyy} + \phi_{y,xxy} \right) \right) \right) \mathrm{d}z \right] \mathrm{d}\zeta - (z-\bar{z}) \left(\sigma xz,x(\bar{z}) + \sigma yz,y(\bar{z}) \right) + \sigma zz(\bar{z}) \end{aligned} \tag{7}$$

where $(\bar{z})$ represents the lower surface, the integral constants must be chosen to fulfill the boundary conditions at the top and bottom surfaces. From Eq. (7) it is possible to notice that the stress recovery strategy requires the estimated values of the third derivative of the displacements and rotation (u, v, ϕ_x, ϕ_y), this can be achieved by different methods.The use of a third-order Lagrange approximation for the displacements $(u, v, w, \phi_x, \phi_y)$ allows for all the terms to be evaluated through interpolation.

Finite Element

Using the Principle of Virtual Displacements the weak form of the FSDT is given by:

$$\begin{aligned} 0 &= \int_{\Omega^e} \left(\frac{\partial \delta u}{\partial x} N_{xx} + \frac{\partial \delta u}{\partial y} N_{xy} \right) dxdy - \oint_{\Gamma^e} \left(N_{xx} n_x + N_{xy} n_y \right) \delta u ds \\ 0 &= \int_{\Omega^e} \left(\frac{\partial \delta v}{\partial x} N_{xy} + \frac{\partial \delta v}{\partial y} N_{yy} \right) dxdy - \oint_{\Gamma^e} \left(N_{xy} n_x + N_{yy} n_y \right) \delta v ds \\ 0 &= \int_{\Omega^e} \left[\frac{\partial \delta w}{\partial x} Q_x + \frac{\partial \delta w}{\partial y} Q_y + \frac{\partial \delta w}{\partial x} \left(N_{xx} \frac{\partial w}{\partial x} + N_{xy} \frac{\partial w}{\partial y} \right) + \frac{\partial \delta w}{\partial y} \left(N_{xy} \frac{\partial w}{\partial x} + N_{yy} \frac{\partial w}{\partial y} \right) - \delta w q \right] dxdy \\ &\quad - \oint_{\Gamma^e} \left[\left(Q_x + N_{xx} \frac{\partial w}{\partial x} + N_{xy} \frac{\partial w}{\partial y} \right) n_x + \left(Q_y + N_{xy} \frac{\partial w}{\partial x} + N_{yy} \frac{\partial w}{\partial y} \right) n_y \right] \delta w ds \\ 0 &= \int_{\Omega^e} \left(\frac{\partial \delta \phi_x}{\partial x} M_{xx} + \frac{\partial \delta \phi_x}{\partial y} M_{xy} + \delta \phi_x Q_x \right) dxdy - \oint_{\Gamma^e} \left(M_{xx} n_x + M_{xy} n_y \right) \delta \phi_x ds \\ 0 &= \int_{\Omega^e} \left(\frac{\partial \delta \phi_y}{\partial x} M_{xy} + \frac{\partial \delta \phi_y}{\partial y} M_{yy} + \delta \phi_y Q_y \right) dxdy - \int_{\Gamma^e} \left(M_{xy} n_x + M_{yy} n_y \right) \delta \phi_y ds \end{aligned} \tag{8}$$

where the n and s index refer to the edges normal and tangential direction components. As discussed before the displacements and rotations will be approximated by:

$$\begin{aligned} u(x,y) &= \sum_{j=1}^{16} u_j \psi_j(x,y), \quad v(x,y) = \sum_{j=1}^{16} v_j \psi_j(x,y), \quad w(x,y) = \sum_{j=1}^{16} w_j \psi_j(x,y) \\ \phi_x(x,y) &= \sum_{j=1}^{16} S_j \psi_j(x,y), \quad \phi_y(x,y) = \sum_{j=1}^{16} S_j \psi_j(x,y) \end{aligned} \tag{9}$$

the ψ_j Lagrange interpolation functions for a Bicubic Element on the local coordinates are defined as:

$$\begin{aligned} \psi_j &= \frac{81}{256}\left(1+\xi^i\xi\right)\left(1+\eta^i\eta\right)\left(\frac{1}{9}-\xi^2\right)\left(\frac{1}{9}-\eta^2\right) && \text{for j =1,4,7,10} \\ \psi_j &= \frac{243}{256}\left(1-\xi^2\right)\left(\eta^2-\frac{1}{9}\right)\left(\frac{1}{3}+3\xi^i\xi\right)\left(1+\eta^i\eta\right) && \text{for j =2,3,8,9} \\ \psi_j &= \frac{243}{256}\left(1-\eta^2\right)\left(\xi^2-\frac{1}{9}\right)\left(\frac{1}{3}+3\eta^i\eta\right)\left(1+\xi^i\xi\right) && \text{for j =5,6,11,12} \\ \psi_j &= \frac{729}{256}\left(1-\xi^2\right)\left(1-\eta^2\right)\left(\frac{1}{3}+3\xi^i\xi\right)\left(\frac{1}{3}+3\eta^i\eta\right) && \text{for j =14,13,15,16} \end{aligned} \tag{10}$$

the nodal points are represented on Fig.3.

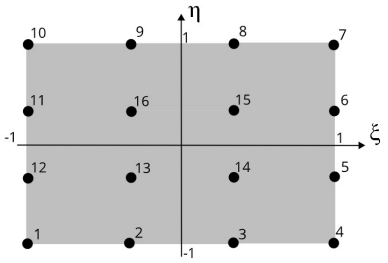

Figure 3 – Simply-supported plate with sinusoidal load.

We can now replace the dependent variables $(u, v, w, \phi_x, \phi_y)$ on Eq. (8) by the third-order Lagrange approximation on Eq. (9) to get the Finite Element:

$$\begin{bmatrix} \mathbf{K}^{11} & \mathbf{K}^{12} & \mathbf{K}^{13} & \mathbf{K}^{14} & \mathbf{K}^{15} \\ \mathbf{K}^{21} & \mathbf{K}^{22} & \mathbf{K}^{23} & \mathbf{K}^{24} & \mathbf{K}^{25} \\ \mathbf{K}^{31} & \mathbf{K}^{32} & \mathbf{K}^{33} & \mathbf{K}^{34} & \mathbf{K}^{35} \\ \mathbf{K}^{41} & \mathbf{K}^{42} & \mathbf{K}^{43} & \mathbf{K}^{44} & \mathbf{K}^{45} \\ \mathbf{K}^{51} & \mathbf{K}^{52} & \mathbf{K}^{53} & \mathbf{K}^{54} & \mathbf{K}^{55} \end{bmatrix} \begin{Bmatrix} \mathbf{u}^e \\ \mathbf{v}^e \\ \mathbf{w}^e \\ \mathbf{S}^1 \\ \mathbf{S}^2 \end{Bmatrix} = \begin{Bmatrix} \mathbf{F}^1 \\ \mathbf{F}^2 \\ \mathbf{F}^3 \\ \mathbf{F}^4 \\ \mathbf{F}^5 \end{Bmatrix} \tag{11}$$

where the stiffness K^{ij} terms and the force terms F^i with $(i,j) = 1,2,...,5$ are given by:

$$
\begin{aligned}
K_{ij}^{11} &= \int_{\Omega^e} \left(A_{11} \frac{\partial \psi_i^{(1)}}{\partial x} \frac{\partial \psi_j^{(1)}}{\partial x} + A_{66} \frac{\partial \psi_i^{(1)}}{\partial y} \frac{\partial \psi_j^{(1)}}{\partial y} \right) dxdy \quad K_{ij}^{12} = \int_{\Omega^e} \left(A_{12} \frac{\partial \psi_i^{(1)}}{\partial x} \frac{\partial \psi_j^{(1)}}{\partial y} + A_{66} \frac{\partial \psi_i^{(1)}}{\partial y} \frac{\partial \psi_j^{(1)}}{\partial x} \right) dxdy \\
K_{ij}^{13} &= \frac{1}{2} \int_{\Omega^e} \left[\frac{\partial \psi_i^{(1)}}{\partial x} \left(A_{11} \frac{\partial w}{\partial x} \frac{\partial \psi_j^{(2)}}{\partial x} + A_{12} \frac{\partial w}{\partial y} \frac{\partial \psi_j^{(2)}}{\partial y} \right) + A_{66} \frac{\partial \psi_i^{(1)}}{\partial y} \left(\frac{\partial w}{\partial x} \frac{\partial \psi_j^{(2)}}{\partial y} + \frac{\partial w}{\partial y} \frac{\partial \psi_j^{(2)}}{\partial x} \right) \right] dxdy \\
K_{ij}^{22} &= \int_{\Omega^e} \left(A_{66} \frac{\partial \psi_i^{(1)}}{\partial x} \frac{\partial \psi_j^{(1)}}{\partial x} + A_{22} \frac{\partial \psi_i^{(1)}}{\partial y} \frac{\partial \psi_j^{(1)}}{\partial y} \right) dxdy \\
K_{ij}^{23} &= \frac{1}{2} \int_{\Omega^e} \left[\frac{\partial \psi_i^{(1)}}{\partial y} \left(A_{12} \frac{\partial w}{\partial x} \frac{\partial \psi_j^{(2)}}{\partial x} + A_{22} \frac{\partial w}{\partial y} \frac{\partial \psi_j^{(2)}}{\partial y} \right) + A_{66} \frac{\partial \psi_i^{(1)}}{\partial x} \left(\frac{\partial w}{\partial x} \frac{\partial \psi_j^{(2)}}{\partial y} + \frac{\partial w}{\partial y} \frac{\partial \psi_j^{(2)}}{\partial x} \right) \right] dxdy \\
K_{ij}^{31} &= \int_{\Omega^e} \left[\frac{\partial \psi_i^{(2)}}{\partial x} \left(A_{11} \frac{\partial w}{\partial x} \frac{\partial \psi_j^{(1)}}{\partial x} + A_{66} \frac{\partial w}{\partial y} \frac{\partial \psi_j^{(1)}}{\partial y} \right) + \frac{\partial \psi_i^{(2)}}{\partial y} \left(A_{66} \frac{\partial w}{\partial x} \frac{\partial \psi_j^{(1)}}{\partial y} + A_{12} \frac{\partial w}{\partial y} \frac{\partial \psi_j^{(1)}}{\partial x} \right) \right] dxdy \\
K_{ij}^{32} &= \int_{\Omega^e} \left[\frac{\partial \psi_i^{(2)}}{\partial x} \left(A_{12} \frac{\partial w}{\partial x} \frac{\partial \psi_j^{(1)}}{\partial y} + A_{66} \frac{\partial w}{\partial y} \frac{\partial \psi_j^{(1)}}{\partial x} \right) + \frac{\partial \psi_i^{(2)}}{\partial y} \left(A_{66} \frac{\partial w}{\partial x} \frac{\partial \psi_j^{(1)}}{\partial x} + A_{22} \frac{\partial w}{\partial y} \frac{\partial \psi_j^{(1)}}{\partial y} \right) \right] dxdy \\
K_{ij}^{34} &= \int_{\Omega c} A_{55} \frac{\partial \psi_i^{(2)}}{\partial x} \psi_j^{(3)} dxdy, K_{ij}^{35} = \int_{\Omega^e} A_{44} \frac{\partial \psi_i^{(2)}}{\partial y} \psi_j^{(3)} dxdy \\
K_{ij}^{44} &= \int_{\Omega^e} \left(D_{11} \frac{\partial \psi_i^{(3)}}{\partial x} \frac{\partial \psi_j^{(3)}}{\partial x} + D_{66} \frac{\partial \psi_i^{(3)}}{\partial y} \frac{\partial \psi_j^{(3)}}{\partial y} + A_{55} \psi_i^{(3)} \psi_j^{(3)} \right) dxdy \\
K_{ij}^{45} &= \int_{\Omega =} \left(D_{12} \frac{\partial \psi_i^{(3)}}{\partial x} \frac{\partial \psi_j^{(3)}}{\partial y} + D_{66} \frac{\partial \psi_i^{(3)}}{\partial y} \frac{\partial \psi_j^{(3)}}{\partial x} \right) dxdy \quad K_{ij}^{55} = \int_{\Omega^c} \left(D_{66} \frac{\partial \psi_i^{(3)}}{\partial x} \frac{\partial \psi_j^{(3)}}{\partial x} + D_{22} \frac{\partial \psi_i^{(3)}}{\partial y} \frac{\partial \psi_j^{(3)}}{\partial y} + A_{44} \psi_i^{(3)} \psi_j^{(3)} \right) dxdy \\
K_{ij}^{33} &= \int_{\Omega^e} \left(A_{55} \frac{\partial \psi_i^{(2)}}{\partial x} \frac{\partial \psi_j^{(2)}}{\partial x} + A_{44} \frac{\partial \psi_i^{(2)}}{\partial y} \frac{\partial \psi_j^{(2)}}{\partial y} + k \psi_i^{(2)} \psi_j^{(2)} \right) dxdy + \frac{1}{2} \int_{\Omega^*} \left\{ \left[A_{11} \left(\frac{\partial w}{\partial x} \right)^2 + A_{66} \left(\frac{\partial w}{\partial y} \right)^2 \right] \frac{\partial \psi_i^{(2)}}{\partial x} \frac{\partial \psi_j^{(2)}}{\partial x} \right. \\
&\quad \left. + \left[A_{66} \left(\frac{\partial w}{\partial x} \right)^2 + A_{22} \left(\frac{\partial w}{\partial y} \right)^2 \right] \frac{\partial \psi_i^{(2)}}{\partial y} \frac{\partial \psi_j^{(2)}}{\partial y} + (A_{12} + A_{66}) \frac{\partial w}{\partial x} \frac{\partial w}{\partial y} \left(\frac{\partial \psi_i^{(2)}}{\partial x} \frac{\partial \psi_j^{(2)}}{\partial y} + \frac{\partial \psi_i^{(2)}}{\partial y} \frac{\partial \psi_j^{(2)}}{\partial x} \right) \right\} dxdy \\
&\quad - \int_{\Omega^e} \left(N_{xx}^T \frac{\partial \psi_i^{(2)}}{\partial x} \frac{\partial \psi_j^{(2)}}{\partial x} + N_{yy}^T \frac{\partial \psi_i^{(2)}}{\partial y} \frac{\partial \psi_j^{(2)}}{\partial y} \right) dxdy
\end{aligned}
\tag{12}
$$

$$
\begin{aligned}
F_i^1 &= \oint_{\Gamma^c} \bar{N}_{nn} \psi i^{(1)} ds, \quad F_i^2 = \oint_{\Gamma^e} \bar{N}_{ns} \psi i^{(1)} ds \\
F_i^3 &= \int_{\Omega^e} q \psi_i^{(2)} dxdy + \oint_{\Gamma^e} Q_n \psi_i^{(2)} ds, \quad F_i^4 = \oint_{\Gamma^c} \bar{M}_{nn} \psi i^{(3)} ds \\
F_i^5 &= \oint_{\Gamma^c} \bar{M}_{ns} \psi i^{(3)} ds, \quad F_i^{1T} = \int_{\Omega^c} \frac{\partial \psi_i^{(1)}}{\partial x} N_{xx}^T dxdy, \quad F_i^{2T} = \int_{\Omega^c} \frac{\partial \psi_i^{(1)}}{\partial y} N_{yy}^T dxdy \\
F_i^{4T} &= \int_{\Omega^e} \frac{\partial \psi_i^{(3)}}{\partial x} M_{xx}^T dxdy, \quad F_i^{5T} = \int_{\Omega^e} \frac{\partial \psi_i^{(3)}}{\partial y} M_{yy}^T dxdy \\
\mathbf{K}^{21} &= \left(\mathbf{K}^{12} \right)^T ; \mathbf{K}^{43} = \left(\mathbf{K}^{34} \right)^T ; \quad \mathbf{K}^{53} = \left(\mathbf{K}^{35} \right)^T ; \quad \mathbf{K}^{54} = \left(\mathbf{K}^{45} \right)^T \\
\mathbf{K}^{14} &= \mathbf{K}^{15} = \mathbf{K}^{24} = \mathbf{K}^{25} = \mathbf{K}^{41} = \mathbf{K}^{42} = \mathbf{K}^{51} = \mathbf{K}^{52} = 0
\end{aligned}
\tag{13}
$$

RESULTS

In order to solve the problems here proposed, the meshes were created utilizing the GID pre-processor software, the FEM evaluation was done using Fortran 2003 and the post-processing was made on Paraview and MATLAB. For the linear problems a third order

approximation was used, to prevent locking effects and recover the out-of-plane stresses. For the Non-linear example a second order approximation was used, for validation purposes and reduced integration was used to prevent locking effects, all of the terms containing the non-linear terms and the Shear stifnesses were integrated using reduced integration. To solve the non-linear system of equations Newtons Iteration Procedure was utilized. For all analysis a shear correction factor $K_s = 5/6$ was utilized.

Linear Stress Recovery

To validate the capabilities of the FSDT to model low span-to-thickness ratio plates, and the stress recovery procedure, we used the analytical 3D linear elasticity of a simply supported plate proposed by Pagano (1970). The plate is submitted to a sinusoidal load of the form:

$$q_0 = \sigma_0 sin\left(\frac{\pi x}{Sh}\right) sin\left(\frac{\pi y}{Sh}\right) \tag{14}$$

where $\sigma_0 = 1$ MPa, S is the span-ratio and h is the plate thickness. A symmetrical laminated plate of 11 layers (equal thickness) is considered here with a cross-ply distribution of $90^\circ/0^\circ$ stacking sequence from the bottom to the top of the plate. The material properties for a plate of a 0° oriented layer are given by:

Table 1 – Mechanical Properties of a 0° oriented plate

E_x [GPa]	E_y, E_z [GPa]	G_{yz} [GPa]	G_{xz}, G_{xy} [GPa]	ν_{yz}, ν_{xz}, ν_{xy}
25.0	1.0	0.2	0.5	0.25

On Fig.4 we have a representation of the problem:

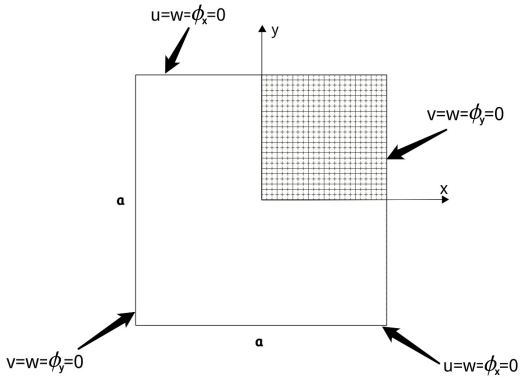

Figure 4 – Simply-supported plate with sinusoidal load.

To solve this problem a symmetry condition was used to reduced computational cost, the boundary conditions utilized were: $\mathbf{u = w = \phi_x = 0}$ at $\mathbf{y = a/2}$, $\mathbf{v = w = \phi_y = 0}$ at $\mathbf{x = a/2}$, $\mathbf{u = \phi_x = 0}$ at $\mathbf{x = 0}$ and $\mathbf{v = \phi_y = 0}$ at $\mathbf{y = 0}$. The length of the plate sides is represented by $\mathbf{a = 22}$ cm. To solve the problem a mesh of 8x8 cubic elements with 16 nodes was used, the stress was then recovered at $\mathbf{x = y = 25a/32}$. The stress results are normalized by:

$$(\bar{\sigma}_{xx}, \bar{\sigma}_{yy}, \bar{\sigma}_{xy}) = \frac{(\sigma_{xx}, \sigma_{yy}, \sigma_{xy})}{\sigma_0 S^2}, \quad (\bar{\tau}_{xz}, \bar{\tau}_{yz}) = \frac{(\tau_{xz}, \tau_{yz})}{\sigma_0 S}, \quad \bar{\sigma}_{zz} = \frac{\sigma_{zz}}{\sigma_0} \tag{15}$$

On Fig.5 the stress field for a plate with span-ratio of $S = 10$ was obtained, it can be seen that the FSDT can still estimate the in plane stresses quite well, with the relative error under 5%. For the out of plane normal stress the recovery result is almost exact and the out of plane shear stress error still is kept under 5%. The other stress field represented on Fig.5 is for a plate with a span-ratio of $\mathbf{S = 5}$, the linear elasticity solutions starts to show the limit of the plate theory assumptions. This is especially true for the in plane shear stress that presents a 25% maximum error at $\mathbf{z = h/2}$, while the normal stress keeps at 10%. The out of plane normal stress starts to deviate, and the shear is kept at 10%.

In order to further investigate the effectiveness of the stress recovery, the procedure was applied on a free edge plate (at $\mathbf{x = y = a/2}$) represented at Fig.6, where $\mathbf{a = 22}$ cm, with a span-ratio of $\mathbf{S = 10}$. The properties are the same of the previous example, but a uniform load was applied. As it can be seen on Fig.7 the stress recovery of the out of plane normal stress converges better at elements further

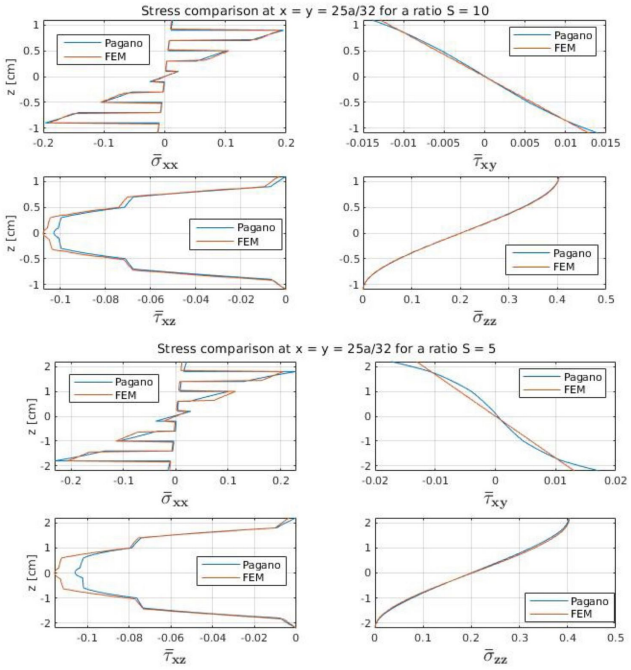

Figure 5 – Stress comparison at $\mathbf{x = y = 25a/32}$ for different $\mathbf{S}$ ratios.

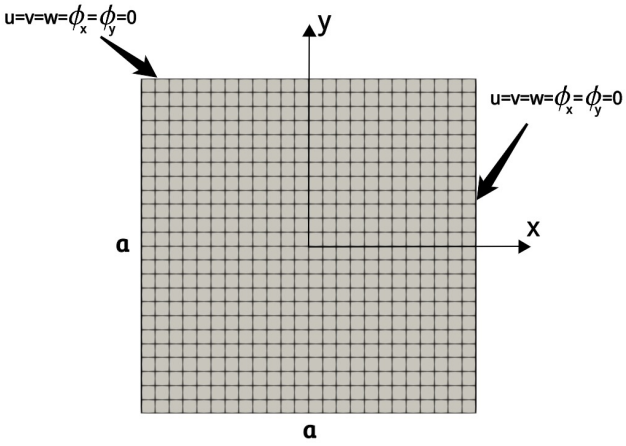

Figure 6 – Plate clamped at $\mathbf{y = x = 0.11}$ m.

from the constrains of the plate, since the boundary condition on the upper surface is the load $q_0 = 10^6$ MPa.

Modified Tsai-Wu critrion

The main focus of the paper is to obtain the out-of-plane stresses in order to model the interlaminar failure with the use of the plate theories. Naik, Gillespie and Eduljee (2019) define a Modified Tsai-Wu Failure Criteria, which assumes that only interlaminar components between the fibers and the composites matrix interact to cause interlaminar failure and the in-plane stresses have a negligible influence. So the criteria is simplified to:

$$F_3\sigma_{zz} + F_{33}\sigma_{zz}^2 + F_{44}\tau_{yz}^2 + F_{55}\tau_{xz}^2 = 1 \tag{16}$$

$$F_3 = \frac{1}{S_{zzt}} + \frac{1}{S_{zzc}}, \qquad F_{33} = \frac{-1}{S_{zzt}S_{zzc}}, \quad F_{44} = \frac{1}{S_{yz}^2}, \quad F_{55} = \frac{1}{S_{xz}^2} \tag{17}$$

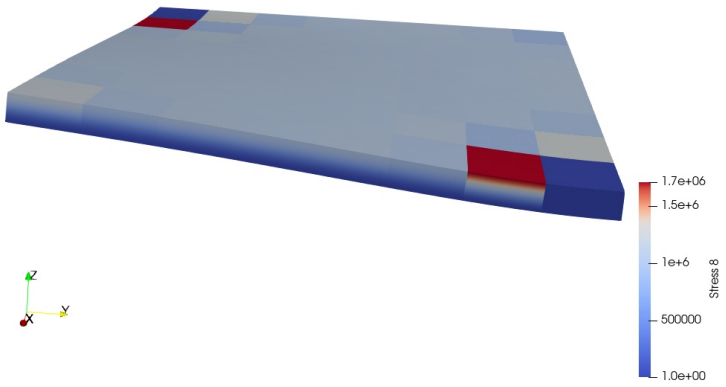

Figure 7 – Transverse normal stress (σ_{zz}) [Pa] recovery for a free edge plate.

where $(S_{zzt}, S_{zzc}, S_{xz}, S_{yz})$ are the tension, compression and shear(xz-plane and yz-plane) interlaminar strengths. For the example represented by Fig.8 the material analyzed is the Carbon-Epoxy composite with the properties:

Table 2 – Carbon-Epoxy Mechanical Properties

E_x [GPa]	E_y [GPa]	G_{yz} [GPa]	ν_{xy}	S_{zzt} [MPa]	S_{zzc} [MPa]	S_{yz}, S_{xz} [MPa]
139.2	8.076	5	0.324	25	-843.3	62.1

In order to analyse stress concentration a plate with a circular hole was used under a uniform load $q0 = 1$ MPa, and a span-ratio $S = 10$ and 3 layers of Carbon-Epoxy on a $90^\circ/0^\circ/90^\circ$ disposition. Fig.8 shows the boundary conditions utilized.

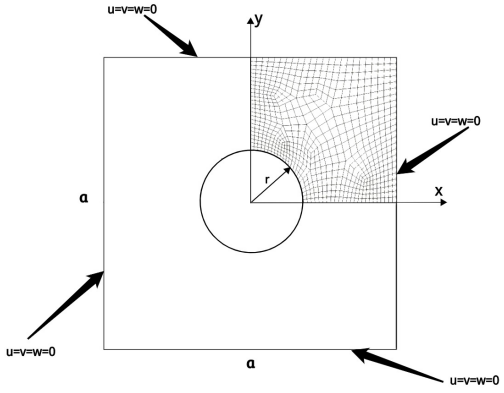

Figure 8 – Simply supported plate with a hole, $\mathbf{u = \phi_x = 0}$ at $\mathbf{x = 0}$ and $\mathbf{v = \phi_y = 0}$ at $\mathbf{y = 0}$. .

Figure 9 shows us the result of the interlaminar failure analysis, as expected the analysis shows us a stress concentration near the plates hole near the center of the plate where the out of plane shear stress is higher.

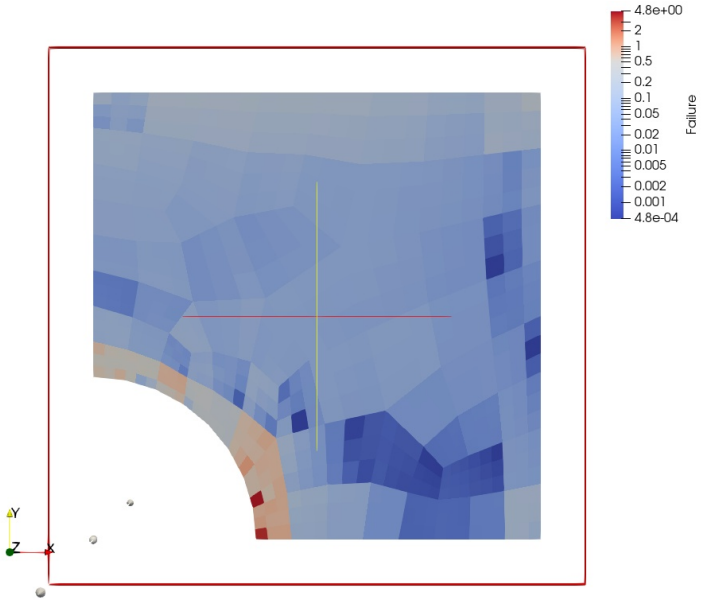

Figure 9 – Modified Tsai-Wu criterion for interlaminar failure for a plate with a hole at $z = 0$, highest failure point.

Non-linear Bending of a Circular Plate

To validate the nonlinear analysis of the Algorithm created, the example represented by Fig.10 proposed by Reddy (2014) was solved. Figure 10a shows a clamped circular isotropic plate of thickness $h = 10$ in, radius $a = 100$ in, Poisson coefficient $v = 0.3$, and Modulus of Elasticity $E = 10^6$ psi. A step-load approach $\Delta q_0 = 25$ psi was used to better convergence.

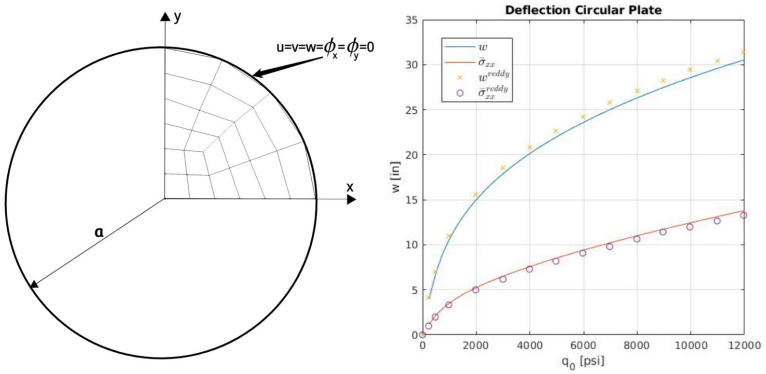

Figure 10 – a) Circular clamped plate, $\mathbf{u = \phi_x = 0}$ at $\mathbf{x = 0}$ and $\mathbf{v = \phi_y = 0}$ at $\mathbf{y = 0}$. b) Non-linear deflection for a circular plate.

Figure 10b shows us that the stress and deflection, calculated at the center of the plate, of the algorithm check with Reddys (2014) solution, with a small divergence, probably related to mesh differences. From Fig.10b it can also be seen the non-linearity of both deflection and normal stress as the load increases.

CONCLUSION

The Reissner-Mindlin plate theory was able to model thick plates with span-ratios down to 10 with excellent results, for lower ratios a more in depth analysis may be necessary. The stress recovery procedure enabled the use of a interlaminar failure criteria. The stress recovery procedure was successful with good results far from stress concentrations. The algorithm was able to obtain the displacement and in-plane stresses for a non-linear plate analysis, which can be further used in a non-linear stress recovery method.

REFERENCES

Hartman, T. B., Hyer, M. W., Case, S. W. (2012). Geometrically nonlinear stress recovery in composite laminates. AIAA journal, 50(5), 1156-1168.

Naik, R. A., Gillespie, JR. J. W., and Eduljee, R. F., 2019. "Development of a modified Tsai-Wu Criterion for Interlaminar Failure in Composite Laminates". Proceedings of the Eighth Japan-US Conference on Composite Mate- rials, p. 639-648.

Pagano, N. J. (1970). Exact solutions for rectangular bidirectional composites and sandwich plates. Journal of Composite Materials (4)1: 20.

Patton, A. et al.,2021. "Accurate equilibrium-based interlaminar stress recovery for isogeometriclaminated composite Kirchhoff plates". Composite Structures, Vol. 256, p. 1-15.

Reddy, J. N. (2004). Mechanics of laminated composite plates and shells: theory and analysis. CRC.

Reddy, J. N. An introduction to nonlinear finite element analysis : with applications to heat transfer, fluid mechanics, and solid mechanics. Oxford: Oxford University Press, 2014.

RESPONSIBILITY NOTICE

The authors are the only parties responsible for the printed material included in this paper.